SPIN DYNAMICS SIMULATIONS AT AGS

H. Huang*, W. W. MacKay*, F. Méot†, T. Roser*
* Collider-Accelerator Department, BNL, Upton, NY 11973, USA
† CEA&IN2P3, LPSC, Grenoble, France

Abstract

To preserve proton polarization through acceleration, it is important to have a correct model of the process. It has been known that with the insertion of the two helical partial Siberian snakes in the Alternating Gradient Synchrotron (AGS), the MAD model of AGS can not deal with a field map with offset orbit. The stepwise ray-tracing code Zgoubi provides a tool to represent the real electromagnetic fields in the modeling of the optics and spin dynamics for the AGS. Numerical experiments of resonance crossing, including spin dynamics in presence of the snakes and Q-jump, have been performed in AGS lattice models, using Zgoubi. This contribution reports on various results so obtained.

INTRODUCTION

In order to overcome the spin depolarizing resonances, partial snakes [1] have been employed in the AGS during the polarized proton acceleration. With the two partial snakes in the AGS, all vertical intrinsic resonances and imperfection resonance conditions are avoided. To understand the residual polarization loss during acceleration, the spin numerical simulation has been done before but recently a new series of simulations for the AGS have been performed with the ray-tracing Zgoubi [2], that has proven to be efficient in that matter [3].

Spin dynamics simulations include : 1) crossing and neighboring of spin resonances ; 2) dynamics in presence of the two helical snakes ; 3) Q-jump. The AGS bare lattice is considered here, including sextupole components in the combined function main bends, exclusive of other nonlinearities as fringe fields, comprised of the two helical snakes where relevant. There are a series of goals in these numerical experiments, including : 1) assessing and checking the capabilities of the numerical code ; 2) performing comparisons with other existing methods [4] ; 3) extending spin dynamics investigations in relation with AGS, based on Zgoubi capabilities ; 4) producing new results ; 5) allowing further comparison with, and further planning of, numerical experiments.

In the following, the working hypotheses are first recalled : AGS lattice, snakes, etc., together with the basis of the analytical approach of depolarizing resonance effects to which the text will be referring in due place. The next Section shows typical effects of depolarizing resonance neighboring and crossing, whereas the last Section reports on spin dynamics in the presence of snakes and on Q-jump resonance crossing. These examples, in reduced number here, have been drawn from Technical Notes that expose on numerous simulations, to which the reader may refer for further details [5, 6].

Table 1: AGS parameters.

	MAD8	Ray-tracing
Circumference /m	807.07564	807.04378
Q_x, Q_y	8.7106, 8.7644	[8].7119, [8].7635
Q'_x,Q'_y	-22.734, 1.734	-20.986, 1.794
α, $\sqrt{1/\alpha}$	0.0140, 8.450	0.0140, 8.451
Periodic parameters at "Beginning of AGS" :		
β_x, β_y /m	19.785, 11.701	19.843, 11.675
α_x, α_y	-1.585, 1.037	-1.588, 1.033
D_x /m, D'_x /rad	2.211, 0.154	2.034, 0.144
x_{co} /mm, x'_{co} /mrad	0, 0	-6.43 -0.50

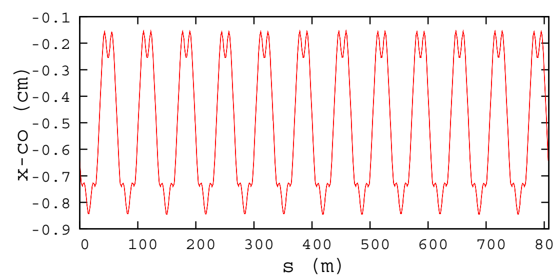

Figure 1: Horizontal closed orbit along the ring.

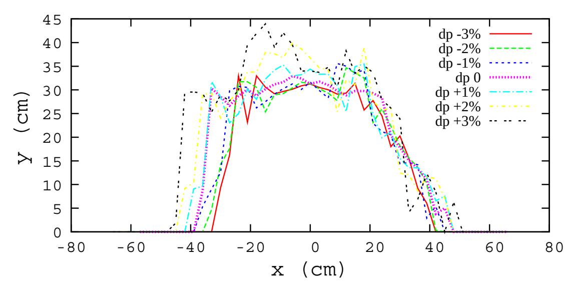

Figure 2: Dynamic apertures, $\delta p/p = 0, \pm 1, \pm 2, \pm 3\%$.

BARE RING, RESONANCE STRENGTHS

LATTICE Tab. 1 displays general optical parameters of the AGS 12-superperiod bare lattice as drawn from the ray-tracing method, with comparison with MAD8 values.

Note the $\approx$ 3.2 cm difference in orbit length, which results from the lattice description in MAD (bends, using 'SBEND', whereas a more realistic representation, 'MULTIPOL', straight axis, is used in Zgoubi). However this effect is of minor importance for the moment. Note also the non-zero closed orbit in Zgoubi, Fig. 1, as induced by the straight axis combined function dipoles. MAD and Zgoubi

Table 2: Intrinsic resonances, $\nu_y = 8.7634$. Strengths from DEPOL are given for comparison.

Systematic, $12k \pm \nu_y$	T	Crossing $A^2/\frac{\epsilon_y}{\pi}$	P_{final}	DEPOL $A^2/\frac{\epsilon_y}{\pi}$
	(GeV)	(10^6)		(10^6)
$0 + \nu_y$	3.648	3.73	-0.052	4.31
$36 - \nu_y$	13.32	11.0	0.155	11.35
$24 + \nu_y$	16.21	0.037	0.857	0.06
$48 - \nu_y$	19.60	0.404	-0.108	0.29
$36 + \nu_y$	22.49	71.6	-0.522	67.21
Random, $k \pm \nu_y$				
$23 + \nu_y$	15.68	0	1.	0

yield identical β_x and β_y betatron functions, however computation of AGS DA at injection (Fig. 2) requires the ray-tracing method.

SPIN In the numerical simulations we take rf voltage $\hat{V} = 290$ kV, synchronous phase $\phi_s = [180-]\,30$ degrees ($\gamma_{tr} = 8.451$, Tab. 1), hence $\Delta E = 145$ keV/turn, then, given proton mass as $M_0 = 938.272$ MeV, anomalous magnetic moment of proton as $G = 1.79285$, and depolarizing resonance crossing speed $\alpha = G\frac{d\gamma}{d\theta} = G\frac{1}{2\pi}\frac{\Delta E}{M_0}$, the crossing speed value is $\alpha = 4.4096\,10^{-5}$. Besides, $\dot{B} = \Delta E\,/\,(2\pi R\rho) = \Delta E\,/\,(\mathcal{C}\rho)$. Given AGS circumference as $\mathcal{C} = 807.043$ m (Tab. 1), and $1/\rho = B/B\rho = 0.01171\,\mathrm{m}^{-1}$, then $\dot{B} = 2.104$ T/s.

When presenting simulation results in Tabs. 2, 3, we refer to the classical formulas, below.

• *Froissart-Stora :* Polarization after crossing a resonance (Fig. 3) is given by

$$P_{final}/P_{initial} = 2\exp(-A^2) - 1 \qquad (1)$$

where $A^2 = \pi|\epsilon|^2/2\alpha$ and ϵ is the resonance strength. A^2 can be computed, cols. 3, 4 in Tabs. 2, 3 respectively.

• *Static case :* A^2 relates to the average value $\bar{S}_y^2$ of the vertical polarization component and to the distance to the resonance $\Delta = \gamma G - (12n - \nu_y)$ via

$$2\alpha A^2/\pi = \Delta^2(1/\bar{S}_y^2 - 1) \qquad (2)$$

(e.g., 1% (resp. 86.6%) depolarization, i.e. $\bar{S}_y = 0.99$, corresponds to $\Delta = \gamma G - n = 7|2\alpha A^2/\pi|$, i.e. an energy band $\pm\delta\gamma = \pm 7|2\alpha A^2/\pi|/G$ (resp. $\Delta = \gamma G - n = \sqrt{3}|2\alpha A^2/\pi|$)). Numerical $\bar{S}_y^2(\Delta)$ data (the average value of S_y oscillation in Fig. 4) can be matched with Eq. 2 (Fig. 5), this yields A^2 and ν_y.

A limited number of resonances have been explored, relevant to the comparisons undertaken with the code DEPOL [4], one of the goals of the present study. It can be observed (Tab. 2) that resonance strength computed from ray-tracing differs from DEPOL's results in some cases of weak resonances, such as $\gamma G = 48 - \nu_y$. In order to assess possible origin of this discrepancy in sextupole components, these have been switched off in all main bends in the bare ring : this practically does not change the results. Work is still needed to understand these differences.

• **Crossing $\gamma G = 48 - \nu_y$ (19.60 GeV) - single particle on** $\epsilon_y/\pi = 0.125\,10^{-6}$

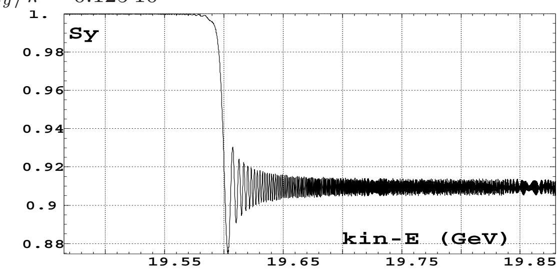

Figure 3: S_y versus kinetic energy.

• **Static, $\gamma G = 48 - \nu_y$ (19.60 GeV) -** $\epsilon_y/\pi = 0.125\,10^{-6}$

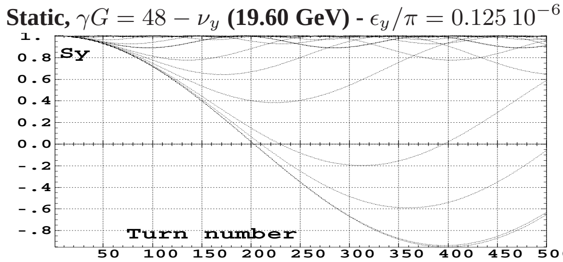

Figure 4: S_y versus turn number for various distances to the resonance.

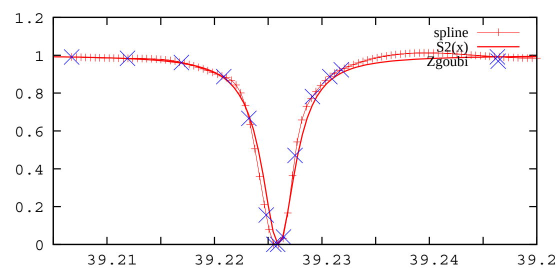

Figure 5: Matching $S_y^2(\Delta)$ (Eq. 2).

Table 3: Closed orbit resonances.

γG	T	$\hat{z}$	$A^2/\hat{z}^2$	P_{final}
	(GeV)	(mm)	(10^6)	
9	3.77180	2.770	0.159	-0.412
12	5.34183	13.84	0.003	0.057
13	5.86517	13.84	0.003	0.158
23	11.0986	13.84	0.905	-0.647
27	13.1920	1.384	0.457	-0.167
45	22.6121	0.275	2.706	0.630

TRACKING WITH SNAKES

Spin dynamics simulations in presence of partial snakes are presented here, more results and details can be found in Ref. [6].

AGS WITH SNAKES AGS is tuned to $\nu_x\,/\,\nu_y = 8.72\,/\,8.98$ in presence of the warm and cold partial snakes.

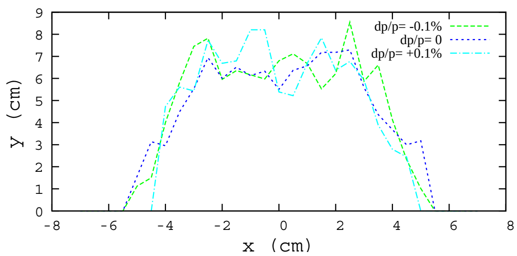

Figure 6: Dynamic apertures in presence of w- and c-snake.

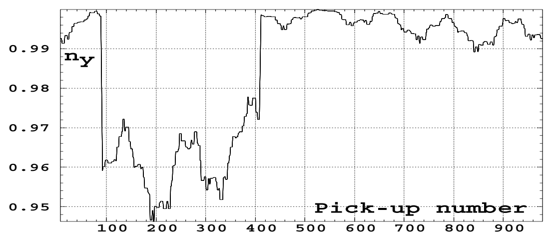

Figure 7: Vertical component of spin $\vec{n}$-vector along the ring at injection energy. The two steps (around PU# 100, 64 m and PU# 400, 330 m) are where the partial snakes locate.

Both snakes are represented by a mid-plane 2-D magnetic field map, from what Zgoubi performs 3-D extrapolation. They introduce both horizontal ($\approx 5 \pm 3$ mm) and vertical ($\approx \pm 4$ mm) closed orbit. The dynamic aperture (Fig. 6) is much reduced compared to the previous settings (Fig. 2). The vertical component of the spin $\vec{n}$-vector in presence of w- and c-snakes, recorded at $\sim$ 990 "pick-ups" along the ring circumference, is displayed in Fig. 7.

Resonance crossing in a first approach is explored by accelerating from $\gamma G = 43.5$ to $\gamma G = 46.5$ so to minimize the closed orbit and higher order effects induced by the snakes. Single particle tracking takes ~ 0.15 second per turn, *real time*, on a 1.3 GHz portable PC hence ~ 50 min for the present 20000-turn run. Acceleration hypotheses with snakes are the same as in the first Section, namely, energy gain $\Delta E = 145$ keV/turn, crossing speed $\alpha = 4.4096\,10^{-5}$, $\dot{B} = 2.104$ T/s, whereas $\phi_s = 150$ degrees.

Acceleration from $\gamma G = 43.5$ to $\gamma G = 46$ requires ~11000 turns, the experiment has been pushed to 20000 turns and $\gamma G = 49$. All resonances in that energy region are imperfection (integer) resonances but for $\gamma G = 36 + \nu_y \approx 44.98$. Spin flip of the vertical spin component S_y of the synchronous particle as observed (in an AGS arc) over the acceleration range is as expected [6], this is discussed further in the next Section.

Q-JUMP Conditions are as above and in addition $\beta\gamma\epsilon_x = 20\pi$ mm.mrad and $\epsilon_y = 0$ at start. A Q-jump scheme is added, causing $\Delta\nu_x = 0.04$, namely $\nu_x : 8.73 \rightarrow 8.77$ (and also $\nu_y : 8.9783 \rightarrow 0.9636$). It uses two quads located at equal $\beta_x = 25$ m, with equal strengths and sum of these $\approx \Delta\nu_x/\beta_x$. Cycling of the two quads is as follows : jumps are centered at +0.25 (ramp up, from zero to full quad strength) and +0.75 (ramp down) from all integer $G\gamma$ values, the jump length is 40 turns. Fig. 8 displays two tracking simulations, superimposed, done with tune jump respectively on and off, condidering 50 particles with initial horizontal coordinates taken in Gaussian distribution while $\epsilon_y = 0$, and initial spin taken on the local $\vec{n}$-vector (close to vertical, see Fig. 7). Fig. 9 shows details ($\nu_s = 35 + \nu_x$ region) of local decrease of S_y oscillations in the presence of tune jump.

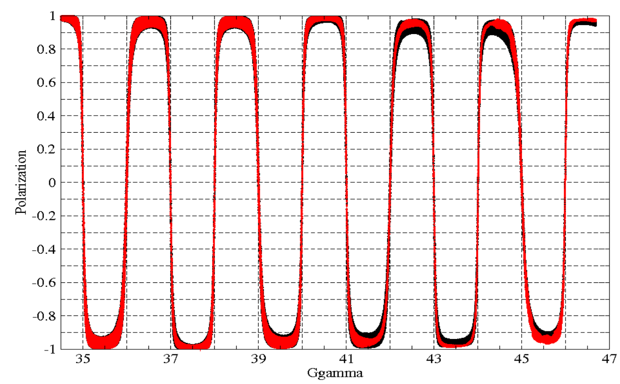

Figure 8: A tracking done for 50 particles. The red trace is with jump quads on, the black trace is with jump quads off.

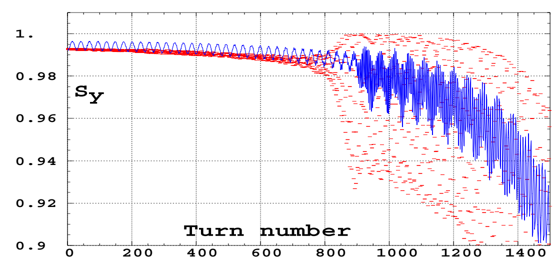

Figure 9: Single particle, effect of the Q-jump. The solid line is for jump quads on which clearly shows less variation and results in better polarization at the end of the acceleration.

CONCLUSION

The stepwise ray-tracing code Zgoubi has been used for simulations of AGS beam optics and spin dynamics. Since it uses real electro-magnetic fields in the simulation, it is more realistic than other codes. It is especially a useful tool when the partial helical snake magnets are included. The code shows that the newly proposed horizontal tune jump method indeed helps polarization preservation.

Acknowledgements The cold snake map was generated by Ramesh Gupta, and the warm map by Masahiro Okamura and Junpei Takano.

REFERENCES

[1] H. Huang, *et al.*, Phys. Rev. Lett. **99**, 154801 (2007).
[2] F. Méot, NIM-A 427 (1999) 353-356.
[3] F. Méot, NIM-A 313 (1992) 492-500.
[4] E. D. Courant, and R. D. Ruth, BNL 51270, Upton (1980).
[5] F. Méot, H. Huang, Int. Report IN2P3/LPSC-10-31 (2009).
[6] F. Méot, H. Huang, Int. Report IN2P3/LPSC-10-32 (2010).